

The indigenous South American Tsimane exhibit relatively modest decrease  
in brain volume with age despite high systemic inflammation

Andrei Irimia, Ph.D.<sup>1, 2\*</sup>, Nikhil N. Chaudhari, M.S.<sup>1</sup>, David J. Robles, M.A.<sup>1</sup>, Kenneth A. Rostowsky, B.S.<sup>1</sup>, Alexander S. Maher, M.S.<sup>1</sup>, Nahian F. Chowdhury, B.S.<sup>1</sup>, Maria Calvillo, M.A.<sup>1</sup>, Van Ngo, B.S.<sup>1</sup>, Margaret Gatz, Ph.D.<sup>3</sup>, Wendy J. Mack, Ph.D.<sup>4</sup>, E. Meng Law, M.D.<sup>5, 6, 7</sup>, M. Linda Sutherland, M.D.<sup>8</sup>, James D. Sutherland, M.D.<sup>8</sup>, Christopher J. Rowan, M.D.<sup>9, 10</sup>, L. Samuel Wann, M.D.<sup>11</sup>, Adel H. Allam, M.D.<sup>12</sup>, Randall C. Thompson, M.D.<sup>13</sup>, David E. Michalik, D.O.<sup>14, 15</sup>, Daniel K. Cummings, Ph.D.<sup>16, 17</sup>, Edmond Seabright, PhD.<sup>16</sup>, Sarah Alami, M.A.<sup>18</sup>, Angela R. Garcia, Ph.D.<sup>19</sup>, Paul L. Hooper, Ph.D.<sup>16</sup>, Jonathan Stieglitz, Ph.D.<sup>20</sup>, Benjamin C. Trumble, Ph.D.<sup>19</sup>, Michael D. Gurven, Ph.D.<sup>18</sup>, Gregory S. Thomas, M.D.<sup>8, 21</sup>, Caleb E. Finch, Ph.D.<sup>1, 22</sup>, and Hillard Kaplan, Ph.D.<sup>17</sup>

<sup>1</sup> Ethel Percy Andrus Gerontology Center, Leonard Davis School of Gerontology, University of Southern California, 3715 McClintock Avenue, Suite 228, Los Angeles CA 90089 USA

<sup>2</sup> Corwin D. Denney Research Center, Department of Biomedical Engineering, University of Southern California, 1042 Downey Way, Los Angeles CA 90089 USA

<sup>3</sup> Center for Economic and Social Research, Dana and David Dornsife College of Letters, Arts and Sciences, University of Southern California, 635 Downey Way, Los Angeles CA 90089 USA

<sup>4</sup> Department of Preventive Medicine, Keck School of Medicine, University of Southern California, 2001 North Soto Street, SSB 202Y, Los Angeles CA 90089 USA

<sup>5</sup> iBRAIN Research Laboratory, Departments of Neuroscience, Computer Systems and Electrical Engineering, Monash University, 99 Commercial Road, Melbourne VIC 3004 Australia

<sup>6</sup> Department of Radiology, The Alfred Health Hospital, 55 Commerce Road, Melbourne VIC 3004 Australia

<sup>7</sup> Department of Neurology, Keck School of Medicine of USC, 1520 San Pablo Street, University of Southern California, Los Angeles CA 90033 USA

<sup>8</sup> MemorialCare Heart & Vascular Institute, 17360 Brookhurst Street, Fountain Valley CA 92708 USA

<sup>9</sup> Renown Institute for Heart and Vascular Health, 1500 East Second Street, Suite 400, Reno NV 89502 USA

<sup>10</sup> School of Medicine, University of Nevada, 1664 North Virginia Street, Reno NV 89557 USA

<sup>11</sup> Ascension Healthcare, 2350 North Lake Drive, Suite 400, Milwaukee, WI 53211 USA

<sup>12</sup> Department of Cardiology, School of Medicine, Al-Azhar University, Al Mikhaym Al Daem, Cairo, Egypt

<sup>13</sup> Saint Luke's Mid America Heart Institute, 4401 Wornall Road, University of Missouri, Kansas City MO 64111 USA

<sup>14</sup> Department of Pediatrics, School of Medicine, University of California at Irvine, Orange CA 92697 USA

<sup>15</sup> MemorialCare Miller Children's & Women's Hospital, Long Beach Medical Center, 2801 Atlantic Avenue, Long Beach CA 90806 USA

<sup>16</sup> Department of Anthropology, MSC01-1040, University of New Mexico, Albuquerque, NM 87131 USA

<sup>17</sup> Economic Science Institute, Argyros School of Business and Economics, Chapman University, 1 University Drive, Orange CA 92866 USA

<sup>18</sup> Department of Anthropology, University of California, Santa Barbara CA 93106 USA

<sup>19</sup> Center for Evolution & Medicine, School of Human Evolution and Social Change, Arizona State University, Life Sciences C, 427 East Tyler Mall, Tempe AZ 85281

<sup>20</sup> Institute for Advanced Study in Toulouse, Toulouse 1 Capitol University, 1 Esplanade de l'Université, 31080 Toulouse Cedex 06, France

<sup>21</sup> Division of Cardiology, University of California, Irvine, Orange CA 92868 USA

<sup>22</sup> Departments of Biological Sciences, Anthropology and Psychology, Dana and David Dornsife College of Letters, Arts and Sciences, University of Southern California, 3551 Trousdale Parkway, Los Angeles CA 90089 USA

\* Materials and correspondence should be addressed to:

Andrei Irimia

Ethel Percy Andrus Gerontology Center

Leonard Davis School of Gerontology

University of Southern California

3715 McClintock Avenue, Suite 228

Los Angeles CA 90089 USA

Telephone: +1 (213) 740-1710

Fax: +1 (213) 740-0792

Email: [irimia@usc.edu](mailto:irimia@usc.edu)

## Abstract

Brain atrophy is correlated with risk of cognitive impairment, functional decline, and dementia. Despite a high infectious disease burden, Tsimane forager-horticulturists of Bolivia have the lowest prevalence of coronary atherosclerosis of any studied population and present few cardiovascular disease (CVD) risk factors despite a high burden of infections and therefore inflammation. This study (A) examines the statistical association between brain volume and age for Tsimane, and (B) compares this association to that of three industrialized populations in the U.S. and Europe. This cohort-based panel study enrolled 746 participants aged 40 to 94 (396 males), from whom computed tomography (CT) head scans were acquired. Brain volume (*BV*) and intracranial volume (*ICV*) were calculated from automatic head CT segmentations.

The linear regression coefficient estimate  $\hat{\beta}_T$  of the Tsimane (*T*), describing the relationship between age (predictor) and *BV* (response, as a percentage of *ICV*), was calculated for the pooled sample (including both sexes) and for each sex.  $\hat{\beta}_T$  was compared to the corresponding regression coefficient estimate  $\hat{\beta}_R$  of samples from the industrialized reference (*R*) countries. For all comparisons, the null hypothesis  $\beta_T = \beta_R$  was rejected both for the combined samples of males and females, as well as separately for each sex. Our results indicate that the Tsimane exhibit a significantly slower decrease in brain volume with age than populations in the U.S. and Europe. Such reduced rates of brain volume decrease, together with a subsistence lifestyle and low cardiovascular disease risk, may protect brain health despite considerable chronic inflammation related to infectious burden.

## Keywords

Brain aging, cardiovascular disease, neurodegeneration.

## Introduction

Ageing-related brain atrophy is strongly associated with elevated risk of cognitive impairment, functional decline, and dementia, and is moderated by factors like diet, smoking and physical activity. Brain atrophy trajectories are positively associated with cardiovascular disease (CVD) risk factors (1) like high cholesterol, diabetes, and hypertension, which are widespread in modern, industrialized populations (2). Thus, populations with a lower prevalence of CVD risk factors are hypothesized to exhibit *slower* brain volume (*BV*) loss and lower risk for associated cognitive decline. On the other hand, populations with high infectious and inflammatory burdens are hypothesized to exhibit *faster* *BV* loss (3, 4) because systemic inflammation predicts greater brain atrophy (5-7).

Indigenous Tsimane forager-horticulturists of lowland Bolivia have a lifestyle similar to that of subsistence populations prior to mechanized agriculture, urbanization and industrialization. The ~16,000 members of this population live by farming, hunting, gathering, and fishing in the Amazon basin, and have a documented high burden of infections and inflammation (8), including increased systemic inflammation (9). This is reflected by their biomarkers of chronic immune activation, including higher leukocytes counts, faster erythrocyte sedimentation rates, and higher levels of C-reactive protein (9), interleukin-6 and immunoglobulin-E (10) than in Americans of all ages (9, 11, 12). The Tsimane feature endemic polyparasitism involving helminths (13) and frequent gastrointestinal illness; most morbidity and mortality in this population being due to infections (9, 14). The higher inflammatory burden among the Tsimane suggests the hypothesis that they exhibit *steeper* negative associations between *BV* and age compared to populations with relatively lower systemic inflammation. Despite their inflammatory load, however, Tsimane have the lowest prevalence of coronary atherosclerosis of any studied population (8) and present few CVD

risk factors like hypertension (15), obesity, type 2 diabetes and hyperlipidemia (16, 17). Additionally, Tsimane have CVD protective factors like high levels of physical activity starting early in life (18), and a diet that is rich in fiber, omega-3 fatty acids and polyunsaturated fatty acids (19), but low in saturated fats and preservatives (20). Thus, to the extent that CVD and cognitive decline risk factors are shared (21), one might hypothesize a shallower negative association between brain volume and age for Tsimane compared to industrialized populations. These divergent hypotheses were tested in this cohort-based panel study.

## Methods

*Study design and participants.* The Tsimane Health and Life History Project (THLHP) team has been studying the Tsimane since 2002, covering 85 villages and sampling persons aged 40 or older in a cohort-based panel design. The team visits Tsimane villages regularly and undertakes clinical examinations to study within- and cross-population variations in aging, including studies of infections and inflammation, coronary atherosclerosis, diet, and physical activity, as described above. The cross-sectional sample of this study includes individuals who self-identified as Tsimane and who were aged between 40 and 94. The Tsimane exhibit a pyramidal population structure, with relatively fewer persons aged over 60. For this reason, all individuals over 60 were screened for enrollment. Potential participants aged 40-59 were identified for screening at the community—rather than individual—level. This approach was adopted for reasons of cultural appropriateness, so that no potential volunteer would feel either targeted or excluded. All Tsimane over 60 participated except for 81 individuals; 9 declined to participate, 17 were not in their home communities at the time of the study, 9 were busy with subsistence activities, one person was hospitalized, and 49 individuals wanted to participate in the future but had prior obligations at the time of scanning. There were no

significant differences in age or sex for participants and non-participants over age 60 (age:  $t_{103} = 1.98$ , Cohen's  $d = 0.27$ ,  $p = 0.95$ ; sex:  $t_{114} = -0.81$ , Cohen's  $d = -0.10$ ,  $p = 0.58$ ). A total of 746 participants (396 males) participated in the study. Included were 143 participants under age 50, 239 between 50 and 59, 226 between 60 and 69, 105 between 70 and 79, 29 between 80 and 89 and 4 aged 90 or above. Participants were compensated for their time.

*CT acquisition.* Participants were bussed to the city of Trinidad, Bolivia, whose CT imaging facility is closest to the Tsimane villages. Although MRI would have been preferable to CT, providing participants with transportation to an MRI scanner facility was not logistically feasible. A licensed radiological technician acquired head CT scans using a 16-detector row scanner (GE BrightSpeed, Milwaukee, WI, USA). At least three team clinicians supervised and reviewed the scans. Images were acquired clockwise, in helical mode, with a standard convolution kernel, and with two reconstructions: one with a voxel size of  $1.25 \text{ mm} \times 1.25 \text{ mm} \times 1.25 \text{ mm}$ , and another with a voxel size of  $0.625 \text{ mm} \times 0.625 \text{ mm} \times 0.625 \text{ mm}$ . Additional parameters included a kilovoltage peak (kVp) of 120 kV, a data collection diameter of 250 mm, a mean exposure time of 1417 ms, an X-ray tube current of 140 mA, and a focal spot of 0.7 mm.

*CT segmentation.* CT volumes were segmented as described extensively elsewhere (22). Briefly, a probabilistic classification method (23) was used to perform tissue classification; voxel intensity values were used to assign their probabilities of belonging to one of several tissue classes by estimating the intensity distributions parameters of each class. The segmentation approach assigns each CT voxel in the cranium to either *BV*, or *CSFV*, such that  $ICV = BV + CSFV$ . The distribution of image intensities was modeled by a mixture of clusters, each consisting of Gaussian random variables (24). By estimating the parameters of

the intensity distributions for each class, voxel intensity information can be used to assign each voxel a probability of belonging to each tissue class. First, an objective function derived from a mixture of Gaussian random variable models is derived, and the value of this function is minimized using a parameter optimization process. *A priori* tissue probability maps specified by an atlas are leveraged to assist this classification. This probabilistic atlas is used to specify the prior probability for each voxel to belong to any tissue class in the Gaussian mixture model. The objective function weighs the probability maps of the atlas using Bayesian inference and then deforms the maps so that they match the volumes to be segmented. At this stage, the atlas template is warped to each subject's brain volume (25), the latter is segmented and the spatial classifications are smoothed (26). Model parameters are optimized using an expectation maximization (EM) algorithm (24), where the Gaussian mixture and deformations are reassessed iteratively and deformations are optimized using a Gauss-Newton scheme (27). When integrated with *a priori* information provided by the template, Bayesian inference facilitates the calculation of posterior probabilities based on each subject's voxel intensities.

**CT-to-MRI validation.** We validated our CT segmentation approach using a sample of 24 US adults aged 54 to 75 who had both MRI and CT scans of the head. In this validation study, CT scan parameters and spatial resolution were like those of the CTs acquired from the Tsimane.  $T_1$ -weighted MRI volumes were acquired at 3 T in a Prisma MAGNETOM Trio TIM scanner (Siemens Corp., Erlangen, Germany) using a magnetization-prepared rapid acquisition gradient echo (MP-RAGE) sequence with the following parameters: repetition time ( $T_R$ ) = 1,950 ms; echo time ( $T_E$ ) = 3 ms; inversion time ( $T_I$ ) = 900 ms; flip angle (FA) = 9 degrees; percentage sampling = 100; pixel bandwidth (BW) = 240 Hz/pixel; matrix size =  $256 \times 256$ ; voxel size = 1 mm  $\times$  1 mm  $\times$  1 mm. In the CT-to-MRI comparison, CT



segmentations were validated against MRI segmentations which had been implemented using Freesurfer 7.0 software, as detailed elsewhere(22). Three quantitative measures were calculated: (A) the Sørensen-Dice coefficient (conveying the overlap between CT and MRI tissue labeling maps), (B) the Hausdorff distance (a measure of how far the CT- and MR-based boundaries are between tissues), (C) the intraclass correlation coefficient (a metric of measurement reproducibility which is useful when distinct techniques are used to measure the same empirical quantity). The Sørensen-Dice coefficient was found to have a Gaussian distribution with mean  $\mu = 89.3\%$  and standard deviation  $\sigma = 0.85\%$  for the brain; for ventricular CSF,  $\mu = 92.2\%$  and  $\sigma = 0.175\%$ . The average Hausdorff distance and its  $\pm 2\sigma$  interval were  $2.1 \pm 0.9$  mm for the brain, and  $2.5 \pm 1.3$  mm for ventricular CSF. The intraclass correlation coefficient was 0.78 for the brain and 0.74 for CSF. Together, these metrics were found to indicate segmentation quality which was adequate for the purpose of *BV* calculations. Across the entire validation sample, the mean percentage difference between CT- and MRI-based volumetrics and its  $\pm 2\sigma$  interval were found to be  $\sim 0\% \pm 3.2\%$  for *BV* and  $\sim 0\% \pm 2.6\%$  for *CSFV*. Thus, on average in this small sample, our CT- and MRI-derived measures differ by a negligible amount, confirming that the CT-based volumetrics can be compared to the MRI-based measures with little average inter-modality error.

*Tsimane comparison to other cohorts.* We compared the Tsimane regression coefficients  $\beta_T$  to those calculated from two MRI studies of aging. The first study, by Schippling *et al.* (28), involved 564 participants scanned in either Hamburg, Germany ( $N = 248$ ) or St. Louis, USA ( $N = 316$ ). This study was included partly because it utilized a segmentation technique for MRI scans similar to ours used for CT scans, which adds to the comparability of  $\beta_T$  and  $\beta_R$ . The second study, by Vinke *et al.* (29), investigated 5,286 participants in the Rotterdam Study, a population-based study of age-related diseases. Both Schippling *et al.* and Vinke *et*

*al.* analyzed MRIs with voxel sizes equal or less than  $1 \text{ mm}^3$ , thus satisfying the typical spatial resolution requirements of today's MRI studies.

For statistical comparison of our *BV* trajectories to those of Schippling *et al.* and Vinke *et al.*, we compared their slopes using linear models. For Schippling *et al.*, who had provided regression coefficients for five-year age intervals,  $\beta_R$  was computed as a weighted average over the age interval from 40 to 70 years (yr). Weights equaled the values of the empirical probability density function associated with the ages of Tsimane participants, thereby allowing us to eliminate the potential confounding effect of differences in age distributions across cohorts. For Vinke *et al.*,  $\beta_R$  was calculated based on the volumetric trajectories and data reported in **Figure 1A** and in **Table 3** of this publication. The volumetric trajectories of Vinke *et al.* are approximately linear within the age intervals [45, 70] yr and [70, 95] yr. Within each of these intervals,  $\beta_R$  is therefore well approximated by  $\Delta V / \Delta t = [V(a_2) - V(a_1)] / (a_2 - a_1)$ , i.e., by the difference in volume  $V$  divided by the difference in age  $a$  across the interval from  $a_1$  to  $a_2$ . The value of  $\beta_R$  within the full interval [45, 95] yr was calculated as the average value of  $\Delta V / \Delta t$  over the intervals [45, 70] yr and [70, 95] yr. Although neither reference study reports their model parameters, both report nonlinear relationships with age. For this reason, we explore nonlinear (quadratic) models for illustration (**Figure 1B**); the reader is referred to the study of Irimia (30) for further quantitation, comparison and meta-analysis of both linear and nonlinear models for *BV*, *WMV*, *GMV* and *CSFV*.

To gain insight into potential neuroanatomic differences between the Tsimane and the reference populations as a function of age, three representative Tsimane female subjects (ages: 40, 60 and 80 yr, respectively) were selected. Three CT scan slices (axial, sagittal, and

coronal) from each subject were collated for illustration of typical age effects upon brain features within the sample (**Figure 2**). To highlight how such features can reflect discrepancies between Tsimane and the reference populations, we also selected two Tsimane subjects aged 80, one whose *BV* was closest to the regression line for the Tsimane (see continuous red trace in **Figure 1A**), and another whose *BV* was closest to the regression line for the reference population (see continuous black trace in **Figure 1A**). Although both subjects are Tsimane, the latter subject's brain CT features are representative of the neuroanatomic profile of an 80-yr-old subject in the reference population. The comparison between the two subjects is illustrated in **Figure 3**.

*Statistical analysis.* Ages were centered on their means prior to statistical analysis. We implemented univariate linear regressions to test the null hypothesis that the Tsimane linear regression coefficient  $\beta_T$  describing the association between age (predictor variable) and *ICV*-adjusted *BV* is equal to zero. Two-tailed Welch's *t* tests were used. The significance of sex as a predictor was explored, the age association was tested both across sexes and within each sex group, and the significance of the sex-by-age interaction was investigated. Statistical analyses of Tsimane data were implemented using IBM SPSS software, version 27.

The linear regression coefficients  $\beta_T$  of the Tsimane (describing associations between age and volumetrics) were compared against regression coefficients  $\beta_R$  reported elsewhere (28, 29) for samples from three industrialized countries (Germany, USA, and the Netherlands, see previous subsection). The null hypothesis  $\beta_T = \beta_R$  was tested both within the full age interval [40, 95] yr and within each of the intervals [40, 70] yr and [70, 95] yr. For *BV*, the null hypothesis  $\beta_T = \beta_R$  was tested at a significance threshold  $\alpha$  of 0.05 using Welch's two-

tailed  $t$  test for independent samples with unequal variances. Regression coefficients were assumed to be normally distributed.

The variance estimates of the regression coefficients  $\beta_T$  and  $\beta_R$  were obtained via bootstrapping using 10,000 simulations. In each simulation, a random subsample  $S$  of size 300 was drawn from the set of Tsimane participants' ages, thus allowing  $\sigma(\beta_R)$  to be estimated without the potentially confounding effect of age distribution differences between the Tsimane and the simulated samples. Then, for a simulated set of Western subjects with ages specified by  $S$ ,  $ICV$ -normalized  $BV$  values were simulated, assuming that these volumes were normally distributed with parameters  $\mu$  and  $\sigma$  equal to those reported by each of the two reference studies (i.e., Schippling *et al.* and Vinke *et al.*). In other words, for each reference study, each sample of simulated volumes had the same distribution as those in the reference sample, and the ages of the subjects whose volumes were simulated were those in the subset  $S$  of 300 subjects selected at random from the Tsimane sample. The regression coefficient estimate  $\hat{\beta}_R$  was then calculated for each such realization. After 10,000 realizations we then computed the estimates  $\hat{\mu}(\beta_R)$  and  $\hat{\sigma}(\beta_R)$ , i.e., the estimated parameters of the normally distributed,  $ICV$ -normalized  $BV$  values reported by the reference study in question.

Once  $\mu(\beta_R) \simeq \beta_R$  and  $\sigma(\beta_R)$  had been estimated, the null hypothesis  $\beta_R = \beta_T$  was tested using Welch's  $t$  test. For all simulations, the error of the Tsimane participants' recorded ages was assumed to be normally distributed with zero mean and a worst-case-scenario value of  $\sigma$  equal to 1.5 yr. This assumption was made because Tsimane birth records are occasionally inaccurate by up to 3 yr (31). Similarly, to reflect uncertainties in the accuracy of CT-derived brain segmentations, the measurement error associated with  $BV$  was assumed to be normally distributed ( $\hat{\mu} = 0\%$ ,  $\hat{\sigma} = 0.8\%$ ), corresponding to a measurement error interval  $[-2\hat{\sigma}, 2\hat{\sigma}]$

equal to  $[-3.2, 3.2]$  %, as observed empirically during validation (see also *CT-to-MRI validation*). The approach described above was used to estimate  $\mu(\beta_I)$  and  $\sigma(\beta_I)$  for each reference cohort. Bootstrapping simulations and statistical tests comparing the Tsimane to reference cohorts were implemented in MATLAB 2020a. *Post hoc* statistical power was calculated using G\*Power 3.1.9.4 software. No hierarchical or complex design implementation was applicable to this analysis.

To evaluate the potential effect of mortality selection on the observed relationship between age and BV in the Tsimane, a Cox proportional hazards model was fit to the Tsimane brain CT sample data, including terms accounting for sex, age, and BV as a percentage of intracranial volume (ICV). To estimate the effect of differential mortality, we simulated hypothetical trajectories of brain aging with and without mortality selection. This begins with the cohort of Tsimane under age 60 at scan time and simulates aging and mortality in each subsequent year of life. During each year included in the simulation, each participant's BV atrophies by some specified amount. The expected mortality is then estimated directly from the Cox model and depends on each simulated BV and age in each year. Mortality selection occurs as individuals with smaller brains are more likely to be removed from the sample, thereby increasing the average BV of remaining participants.

## Results

All Tsimane adults aged over 60 yr were invited to enroll, whereas those aged 40-59 were sampled from a subset of representative communities. The study was approved by the University of New Mexico Health Sciences Institutional Review Board (HRRC 07-157; 15-133). After explaining the procedure and risks in the Tsimane language, informed consent was obtained from the Tsimane government, village leadership, and participants. Because

magnetic resonance imaging (MRI) was logistically unfeasible, low radiation-dose computed tomography (CT) head scans were acquired from 746 participants aged 40 to 94 (396 males) who had accepted our invitation for transportation to the nearest CT imaging facility.  $BV$  and  $ICV$  were calculated from automatic head CT segmentations (22). Volumetrics were normalized by  $ICV$  (i.e.,  $BV$  as percent of  $ICV$  was calculated) to alleviate the confounding effect of head size.

The linear regression coefficient estimate  $\hat{\beta}_T$  of the Tsimane ( $T$ ), describing the relationship between age (predictor) and  $BV$  (response, as a percentage of  $ICV$ ), was calculated for the pooled sample (including both sexes) and for each sex.  $\hat{\beta}_T$  was compared to the corresponding regression coefficient estimate  $\hat{\beta}_R$  of samples from three industrialized reference ( $R$ ) countries. Specifically,  $\hat{\beta}_R$  was extracted from two reference MRI studies (28, 29) that were the most methodologically comparable to our CT study, based on criteria related to image processing and quality. Schippling *et al.* (28) had a combined sample ( $N = 564$ ) of healthy volunteers aged 35 to 75 from Hamburg, Germany ( $N = 248$ ) and St. Louis, USA ( $N = 316$ ). Vinke *et al.* (29) studied 5,286 neurologically healthy participants from Rotterdam, the Netherlands. The null hypothesis  $\beta_T = \beta_R$  was tested at a significance threshold  $\alpha$  of 0.05 across each of two distinct age intervals (40 – 70 yr and 70 – 95 yr), and across the combined age interval 40 – 95 yr. Across a variety of functional and cognitive aging indicators, change accelerates around 70 yr (32), which was selected to define the boundary between the former two intervals.

Values of  $\hat{\beta}_T$  are -0.228%/yr for males and -0.200%/yr for females (**Table 1**). The model including both sexes shows a small significant main effect of male sex reducing  $BV$ ; however, the age-by-sex interaction is not significant, indicating that slopes do not differ

significantly by sex. **Figure 1A** shows *ICV*-normalized *BV* and its age-dependent trajectories for Tsimane and for reference samples. On the interval 40 – 70 yr,  $\hat{\beta}_T = -0.171\%/yr$  is significantly shallower than  $\hat{\beta}_R$ , which equals  $-0.307\%/yr$  for Schippling *et al.* and  $-0.225\%/yr$  for Vinke *et al.* (**Table 2**). Strikingly, on the interval 70 – 95 yr, the Rotterdam estimate  $\hat{\beta}_R = -0.507\%/yr$  is almost twice the value of  $\hat{\beta}_T = -0.271\%/yr$ . The null hypothesis  $\beta_T = \beta_R$  was rejected for the entire age interval 40 – 95 yr both for the combined samples of males and females in the two reference MRI studies, as well as separately for each sex (**Table 3**).

**Figure 2** displays axial, sagittal and coronal CT slices from three representative Tsimane female subjects of ages 40, 60 and 80, respectively. Visual comparison of these CT slices reveals progressive aging of the gray matter and white matter (GM and WM; white and yellow arrows, respectively). Neuroanatomical features of GM aging include GM volume loss reflected by gyral shrinking and sulcal widening in regions like the medial frontal lobes (*cf.*, inferior frontal sulci), lateral and medial temporal lobes (*cf.* superior temporal sulci, temporal opercula), parietal lobes (*cf.* parietal opercula), insulae (*cf.* circular sulci), and hippocampal formations. WM aging features include enlargement of the lateral and third ventricles, as well as brain stem atrophy (e.g., at the boundary between the pons and the medulla oblongata, anterosuperior to the olivary nuclei). Cerebellar atrophy reflects both GM and WM loss in this structure.

**Figure 3** highlights typical neuroanatomic differences between Tsimane and the reference populations of Vinke *et al.* This figure displays CT slices from two Tsimane subjects of age 80; one subject's *BV* is closest to the Tsimane regression line (see continuous red trace in **Figure 1A**), whereas the *BV* of the other is closest to the reference regression line (see

continuous black trace in **Figure 1A**). The *BV* of the second subject (who is representative of the reference population) is ~6.5% larger than that of the first subject (who is representative of Tsimane). The comparison highlights the likely typical extent and features of neuroanatomy differences in old age between the Tsimane and the reference population.

The results of the Cox proportional hazards model are summarized in **Table 4**, which implies that, when *BV* increases by 1%, the mortality hazard decreases by about 5% ( $HR = 0.944$ ). Although the effect is not statistically significant ( $p = 0.196$ ), it is large enough to have potential biological significance, thus justifying the simulation already described to estimate differential mortality effects. The results of this simulation suggest that, when accounting for mortality effects, the observed regression coefficient  $\hat{\beta}_T = -0.2163\%/yr$  for individuals with ages in the interval [40, 95] yr (**Table 2**) corresponds to a mortality-adjusted coefficient of  $\hat{\beta}_T = -0.2240\%/yr$ , which is 3.5% more negative than that observed. Similarly, for individuals with ages in the interval [70, 95] yr, accounting for mortality selection implies that the observed regression coefficient  $\hat{\beta}_T = -0.2706\%/yr$  (**Table 2**) should be ~4% more negative, i.e., that the actual *BV* decrease rate  $\hat{\beta}_T$  is about  $-0.281\%/yr$ .

## Discussion

Although our CT segmentation approach (22) was tested, validated, and compared thoroughly to MRI, this study has limitations. The statistical comparison between Tsimane and the studies of European and US samples relies on a comparison between CT-derived and MRI-derived volumes, respectively, rather than on random sampling and matching of participants scanned using the same neuroimaging modality. While different survival biases across Tsimane and reference samples are potential confounds, the small magnitude of the estimated mortality effect on the slope of *BV* as a function of age suggests that mortality



selection alone is unlikely to account for the large differences in brain volume trajectory between Tsimane and reference samples. Nevertheless, because this study is cross-sectional, inferences on within-individual change in brain atrophy with age await longitudinal data. A total of 567 participants (76% of our sample) constituted 80% of the sample studied by Kaplan *et al* (8), and 685 participants (92% of our sample) constituted 52% of the sample of Rowan *et al.* (33). Thus, although our sample is not identical to those of Kaplan *et al.* and Rowan *et al.*, the biometric profiles of the three samples are likely similar insofar as inflammatory, cardiovascular, and metabolic parameters are concerned.

In conclusion, the Tsimane exhibit smaller age-related *BV* declines relative to industrialized populations, suggesting that their low CVD burden (8) outweighs their high, infection-driven inflammatory risk. If (A) the cross-sectional data (which we believe are population-representative of Tsimane adults aged 40 and over) represent well the average life course of individuals and if (B) the Tsimane are representative of the baseline case prior to urbanization, these results suggest a ~70% increase in the rates of age-dependent *BV* decrease accompanying industrialized lifestyles. Despite its limitations, this study suggests that brain atrophy may be slowed substantially by lifestyles associated with very low CVD risk, and that there is ample scope for interventions to improve brain health, even in the presence of chronically high systemic inflammation. Lastly, the slow rate of age-dependent *BV* decrease in the Tsimane raises new questions about dementia, given the role of both infections and vascular factors in dementia risk.

### **Statement of competing interests**

The authors state that they have no perceived or actual competing interest.

## **Funding**

This work was supported by the National Institute on Aging at the National Institutes of Health (RF1 AG 054442 to H.K., C.E.F. and G.S.T.), as well as by the Institute for Advanced Study in Toulouse and the French National Research Agency (A.N.R.) under the Investments for the Future (Investissements d'Avenir) program (ANR-17-EURE-0010 to J.S.).

## **Author contributions**

Authors contributed to study design (A.I., M.G., J.S., B.C.T., M.D.G., G.S.T., C.E.F., H.K.), subject recruitment (D.K.C., E.S., J.S., B.C.T., M.D.G., H.K.), data collection (C.J.R., L.S.W., A.H.A., R.C.T., D.E.M., D.K.C., E.S., S.A., A.R.G., P.L.H., J.S., B.C.T., M.D.G., H.K.), data curation (A.I., N.N.C., M.C., M.L.S., J.D.S., J.S., B.C.T., H.K.) demographic data analysis (M.G., J.S., B.C.T., M.D.G.), neuroimage analysis (A.I., N.N.C., D.J.R., K.A.R., A.S.M., N.F.C., M.C., V.N., E.M.L., H.C.C., M.L.S., J.D.S.), statistical analysis (A.I., N.N.C., D.J.R., K.A.R., A.S.M., N.F.C., V.N., M.G., W.J.M., P.L.H., B.C.T., M.D.G., C.E.F., H.K.), results interpretation (A.I., N.N.C., D.J.R., M.G., W.J.M., J.S., B.C.T., M.D.G., C.E.F., H.K.), and manuscript redaction (A.I., M.G., W.J.M., J.S., B.C.T., M.D.G., G.S.T., C.E.F., H.K.). All authors reviewed and approved the final version of the manuscript.

## Reference List

1. Manolio TA, Kronmal RA, Burke GL, Poirier V, O'Leary DH, Gardin JM, *et al.* Magnetic resonance abnormalities and cardiovascular disease in older adults. The Cardiovascular Health Study. *Stroke*. 1994;**25**:318-327. doi:10.1161/01.str.25.2.318
2. Kim RE, Yun CH, Thomas RJ, Oh JH, Johnson HJ, Kim S, *et al.* Lifestyle-dependent brain change: a longitudinal cohort MRI study. *Neurobiol Aging*. 2018;**69**:48-57. doi:10.1016/j.neurobiolaging.2018.04.017
3. Jefferson AL, Massaro JM, Wolf PA, Seshadri S, Au R, Vasan RS, *et al.* Inflammatory biomarkers are associated with total brain volume: the Framingham Heart Study. *Neurology*. 2007;**68**:1032-1038. doi:10.1212/01.wnl.0000257815.20548.df
4. Marsland AL, Gianaros PJ, Kuan DC, Sheu LK, Krajina K, Manuck SB. Brain morphology links systemic inflammation to cognitive function in midlife adults. *Brain Behav Immun*. 2015;**48**:195-204. doi:10.1016/j.bbi.2015.03.015
5. Sala-Llloch R, Idland AV, Borza T, Watne LO, Wyller TB, Braekhus A, *et al.* Inflammation, amyloid, and atrophy in the aging brain: relationships with longitudinal changes in cognition. *J Alzheimers Dis*. 2017;**58**:829-840. doi:10.3233/JAD-161146
6. Gu Y, Vorburger R, Scarmeas N, Luchsinger JA, Manly JJ, Schupf N, *et al.* Circulating inflammatory biomarkers in relation to brain structural measurements in a non-demented elderly population. *Brain Behav Immun*. 2017;**65**:150-160. doi:10.1016/j.bbi.2017.04.022
7. Hanning U, Roesler A, Peters A, Berger K, Baune BT. Structural brain changes and all-cause mortality in the elderly population-the mediating role of inflammation. *Age (Dordr)*. 2016;**38**:455-464. doi:10.1007/s11357-016-9951-9

8. Kaplan H, Thompson RC, Trumble BC, Wann LS, Allam AH, Beheim B, *et al.* Coronary atherosclerosis in indigenous South American Tsimane: a cross-sectional cohort study. *Lancet*. 2017;**389**:1730-1739. doi:10.1016/S0140-6736(17)30752-3
9. Blackwell AD, Trumble BC, Maldonado Suarez I, Stieglitz J, Beheim BA, Snodgrass JJ, *et al.* Immune function in Amazonian horticulturalists. *Annals of Human Biology*. 2016;**43**:382-396. doi:10.1080/03014460.2016.1189963
10. Blackwell AD, Gurven MD, Sugiyama LS, Madimenos FC, Liebert MA, Martin MA, *et al.* Evidence for a peak shift in a humoral response to helminths: age profiles of IgE in the Shuar of Ecuador, the Tsimane of Bolivia, and the U.S. NHANES. *PLoS Negl Trop Dis*. 2011;**5**:e1218. doi:10.1371/journal.pntd.0001218
11. Gurven M, Kaplan H, Crimmins E, Finch C, Winking J. Lifetime inflammation in two epidemiological worlds: the Tsimane of Bolivia and the United States. *Journal of Gerontology Biological Sciences*. 2008;**63A**:196-199. doi:10.1093/gerona/63.2.196
12. Vasunilashorn S, Finch CE, Crimmins EM, Vikman SA, Stieglitz J, Gurven M, *et al.* Inflammatory gene variants in the Tsimane, an indigenous Bolivian population with a high infectious load. *Biodemography and Social Biology*. 2011;**57**:33-52. doi:10.1080/19485565.2011.564475
13. Blackwell AD, Martin M, Kaplan H, Gurven M. Antagonism between two intestinal parasites in humans: the importance of co-infection for infection risk and recovery dynamics. *Proceedings of the Royal Society of London B: Biological Sciences*. 2013;**280**:20131671. doi:10.1098/rspb.2013.1671
14. Gurven M, Kaplan H, Supa AZ. Mortality experience of Tsimane Amerindians of Bolivia: Regional variation and temporal trends. *American Journal of Human Biology*. 2007;**19**:376-398. doi:10.1002/ajhb.20600

15. Gurven M, Blackwell A, Eid D, Stieglitz J, Kaplan H. Does blood pressure inevitably rise with age? Longitudinal evidence among forager-horticulturalists. *Hypertension*. 2012;**60**. doi:10.1161/HYPERTENSIONAHA.111.189100
16. Kaplan H, Thompson R, Trumble BC, Wann LS, Allam AH, Beheim B, *et al*. Indigenous South American Tsimane demonstrate the lowest levels of coronary atherosclerosis. *Lancet*. 2017;**S0140**:30752-30753. doi:10.1016/S0140-6736(17)30752-3
17. Vasunilashorn S, Crimmins EM, Kim J-K, Winking J, Gurven M, Kaplan H, *et al*. Blood lipids, infection and inflammatory markers in the Tsimane of Bolivia. *Journal of Human Biology*.**22**:731-740. doi:10.1002/ajhb.21074
18. Gurven M, Jaeggi AV, Kaplan H, Cummings D. Physical Activity and Modernization among Bolivian Amerindians. *PLoS ONE*. 2013;**8**:e55679. doi:doi.org/10.1371/journal.pone.0055679
19. Martin MA, Lassek WD, Gaulin SJ, Evans RW, Woo JG, Geraghty SR, *et al*. Fatty acid composition in the mature milk of Bolivian forager- horticulturalists: controlled comparisons with a US sample. *Maternal & child nutrition*. 2012;**8**:404-418. doi:10.1111/j.1740-8709.2012.00412.x
20. Kraft TS, Stieglitz J, Trumble BC, Martin M, Kaplan H, Gurven M. Nutrition transition in 2 lowland Bolivian subsistence populations. *The American journal of clinical nutrition*. 2018;**108**:1183-1195. doi:10.1093/ajcn/nqy250
21. Stefanidis KB, Askew CD, Greaves K, Summers MJ. The effect of non-stroke cardiovascular disease states on risk for cognitive decline and dementia: a systematic and meta-analytic review. *Neuropsychol Rev*. 2018;**28**:1-15. doi:10.1007/s11065-017-9359-z
22. Irimia A, Maher AS, Rostowsky KA, Chowdhury NF, Hwang DH, Law EM. Brain segmentation from computed tomography of healthy aging and geriatric concussion at variable spatial resolutions. *Front Neuroinform*. 2019;**13**:9. doi:10.3389/fninf.2019.00009

23. Ashburner J, Friston KJ. Unified segmentation. *Neuroimage*. 2005;**26**:839-851. doi:10.1016/j.neuroimage.2005.02.018
24. Bishop CM. *Neural networks for pattern recognition*. New York, NY: Oxford University Press; 1995.
25. Collins DL, Holmes CJ, Peters TM, Evans AC. Automatic 3D segmentation of neuro-anatomical structures from MRI. *Human Brain Mapping*. 1995;**3**:190-208. doi:10.1002/hbm.460030304
26. Evans AC, Kamber M, Collins DL, Macdonald D. An MRI-based probabilistic atlas of neuroanatomy. In: Shorvon SD, Fish DR, Andermann F, Bydder GM, Stefan H, eds. *Nato Adv Sci Inst Se*: Springer; 1994:263-274. doi:10.1007/978-1-4615-2546-2\_48
27. Wedderburn RWM. Quasi-likelihood functions, generalized linear-models, and Gauss-Newton method. *Biometrika*. 1974;**61**:439-447. doi:DOI 10.1093/biomet/61.3.439
28. Schippling S, Ostwaldt AC, Suppa P, Spies L, Manogaran P, Gocke C, *et al*. Global and regional annual brain volume loss rates in physiological aging. *J Neurol*. 2017;**264**:520-528. doi:10.1007/s00415-016-8374-y
29. Vinke EJ, de Groot M, Venkatraghavan V, Klein S, Niessen WJ, Ikram MA, *et al*. Trajectories of imaging markers in brain aging: the Rotterdam Study. *Neurobiol Aging*. 2018;**71**:32-40. doi:10.1016/j.neurobiolaging.2018.07.001
30. Irimia A. Cross-sectional volumes and trajectories of the human brain, gray matter, white matter and cerebrospinal fluid in 9473 typically aging adults. *Neuroinformatics*. 2021;**19**:347-366. doi:10.1007/s12021-020-09480-w
31. Gurven M, Kaplan H, Supa AZ. Mortality experience of Tsimane Amerindians of Bolivia: regional variation and temporal trends. *Am J Hum Biol*. 2007;**19**:376-398. doi:10.1002/ajhb.20600

32. Li X, Ploner A, Wang Y, Magnusson PK, Reynolds C, Finkel D, *et al.* Longitudinal trajectories, correlations and mortality associations of nine biological ages across 20-years follow-up. *Elife*. 2020;**9**. doi:10.7554/eLife.51507
33. Rowan CJ, Eskander MA, Seabright E, Rodriguez DE, Linares EC, Gutierrez RQ, *et al.* Very low prevalence and incidence of atrial fibrillation among Bolivian forager-farmers. *Ann Glob Health*. 2021;**87**:18. doi:10.5334/aogh.3252

Accepted Manuscript

## Tables

**Table 1.** Regressions of age and sex (predictor variables) against *ICV*-normalized *BV*

(response variable) in the Tsimane. Intercepts, linear regression coefficient estimates ( $\hat{\beta}_T$ ), standard errors of the mean (SEMs), Student's *t* statistics, 95% confidence intervals (CIs), effect sizes (partial  $\eta^2$ ) and observed power are reported. *BV* and age are significantly associated both when each sex (M, F) is considered separately, and when the sexes are considered together (M&F). Ages were centered on their mean prior to statistical analysis. For all statistical tests, *p*-values are smaller than  $1.0 \times 10^{-3}$ . The age-by-sex interaction was not found to be significant ( $p = 0.234$ ) but the test is underpowered (power = 0.221).

group	variable	$\hat{\beta}_T$	SEM	<i>t</i>	CI	partial $\eta^2$	power
M	intercept	84.801	0.170	499.798	[84.467, 85.134]	0.998	1.000
	age	-0.228	0.016	-13.893	[-0.260, -0.196]	0.327	1.000
F	intercept	85.698	0.170	503.324	[85.363, 86.032]	0.999	1.000
	age	-0.200	0.016	-12.340	[-0.232, -0.168]	0.304	1.000
M&F	intercept	85.698	0.176	486.484	[85.352, 86.043]	0.997	1.000
	age	-0.200	0.017	-11.927	[-0.233, -0.167]	0.160	1.000
	male sex	-0.897	0.241	-3.716	[-1.371, -0.423]	0.018	0.960
	age $\times$ male sex	-0.028	0.023	-1.191	[-0.073, 0.018]	0.002	0.221



**Table 2.** The relationship between age in years (yr, predictor) and *ICV*-normalized *BV* (percentage of *ICV*, response) on the age intervals [40, 70] yr, [70, 95] yr and [40, 95] yr, as described by linear regression coefficient estimates  $\hat{\beta}$  and their confidence intervals (CIs). Aside from values for the Tsimané on the age intervals [40, 70] yr, [70, 95] yr and [40, 95] yr, results are also provided for the reference studies of Schippling *et al.* (28) (on the age interval [40, 70] yr) and Vinke *et al.* (29) (on age intervals [45, 70] yr, [70, 95] yr and [45, 95] yr). Age intervals are in yr; values of  $\beta$  and their CIs are in %/yr. On the age interval [70, 95] yr, the latter two quantities are not provided for the sample of Schippling *et al.* because this study did not include subjects older than 75 yr.

cohort	<i>N</i>	ages	$\hat{\beta}$	CI ( $\hat{\beta}$ )	ages	$\hat{\beta}$	CI ( $\hat{\beta}$ )	ages	$\hat{\beta}$	CI ( $\hat{\beta}$ )
Tsimané	746	[40,	-	[-0.1731, -	[70,	-	[-0.2779, -	[40,	-	[-0.2192, -
		70]	0.1710	0.1689]	95]	0.2706	0.2633]	95]	0.2163	0.2135]
Schippling <i>et al.</i>	564	[40,	-	[-0.3124, -	[70,	—	—	[40,	—	—
		70]	0.3069	0.3014]	95]	—	—	95]	—	—
Vinke <i>et al.</i>	5286	[45,	-	[-0.2281, -	[70,	-	[-0.5106, -	[45,	-	[-0.3683, -
		70]	0.2246	0.2211]	95]	0.5071	0.5036]	95]	0.3649	0.3635]

**Table 3.** Results of testing the statistical null hypothesis  $\beta_T = \beta_R$  using Welch's  $t$  test for samples with unequal variances. The number of degrees of freedom was approximated using the Welch-Satterthwaite equation. Results are reported separately for males (M), females (F) and for combined samples including both males and females (M&F). The null hypothesis was tested for the Tsimane against the samples of both Schippling *et al.* as well as Vinke *et al.* In the latter case, the null hypothesis could only be tested for the combined samples of males and females (M&F) because Vinke *et al.* did not state the numbers of males and females in their sample. Furthermore, because the trajectories of Vinke *et al.* differ substantially across the age intervals [45, 70] and [70, 95], the null hypothesis was tested separately within each of these intervals. In all cases, the threshold for statistical significance is  $\alpha = 0.05$ . All tests have  $p$ -values smaller than  $1.0 \times 10^{-200}$  and power exceeding 99%.

study	Schippling <i>et al.</i>		Vinke <i>et al.</i>					
	[40, 70]		[45, 70]		[70, 95]		[45, 95]	
sex	$t$	$df$	$t$	$df$	$t$	$df$	$t$	$df$
M	-56.99	3961						
F	-81.90	4489						
M&F	-75.47	3388	-60.89	1477	-424.05	1516	-159.05	1469

**Table 4.** Cox proportional hazards model for the Tsimane, including terms for male sex, age, and *BV* as a percentage of *ICV*. The estimated coefficients  $\hat{\beta}$  of the models are reported in addition to hazards ratios (HR) and to *p*-values, for a total of 676 Tsimane (37 deaths).

parameter	$\hat{\beta}$	HR	<i>p</i>
male sex	0.0406	1.501	0.237
age [yr]	0.0995	1.105	<0.001
<i>BV</i> [%]	-0.0577	0.944	0.196

## Figure Captions

**Figure 1. (A)** Cross-sectional brain volume ( $BV$ ) as a percentage of intracranial volume ( $ICV$ ) and its age-dependent linear trajectories in the Tsimane (red), in the reference sample of Schippling *et al.* (blue) and in that of Vinke *et al.* (black). Dots represent Tsimane participants'  $BV$ s. Dash-dotted lines mark the range of trajectories within the confidence interval (CI) of the bootstrapping-estimated regression coefficient estimate  $\hat{\beta}$  (*not* within the CI of the  $BV$  measurements themselves). The Tsimane and reference samples are assumed to have the same mean  $BV$  at ages 40 years (yr), to facilitate comparison of their slopes and to obviate the divergence of trajectories as a function of age. Note the small CIs of  $\hat{\beta}$  across the MRI reference samples and the substantial divergence of the Tsimane CI (red) from it, particularly after age  $\sim 70$  yr. The null hypothesis  $\beta_T = \beta_R$  fails to be accepted both on the interval 40 – 70 yr (Tsimane vs. Schippling *et al.*:  $t_{3388} = -75.47$ ,  $p \approx 1.0 \times 10^{-250}$ , power  $\approx 99\%$ ; Tsimane vs. Vinke *et al.*:  $t_{1477} = -60.89$ ,  $p \approx 1.0 \times 10^{-250}$ , power  $\approx 99\%$ ) and on the interval 70 – 95 yr (Tsimane vs. Vinke *et al.*:  $t_{1516} = -424.05$ ,  $p \approx 1.0 \times 10^{-250}$ , power  $\approx 99\%$ ). **(B)** Like (A), comparing quadratic models of  $BV$  trajectories as a function of age in the Tsimane (red) against quadratic models of the trajectories in Schippling *et al.* (blue) and in Vinke *et al.* (black). CIs and data points for individual Tsimane  $BV$  values are omitted to facilitate comparison. The curvilinear fit to the Tsimane data confirms and reproduces a slower rate of  $BV$  decrease in the Tsimane after age 70, in contrast to the reference samples, where faster rates of cross-sectional  $BV$  decline are observed.

**Figure 2.** Axial, sagittal and coronal CT slices for three representative Tsimane subjects (three females of ages 40, 60 and 80, respectively). Typical aging effects upon the gray matter (GM) and white matter (WM) are highlighted, with WM depicted by semi-transparent

beige overlays superimposed onto the CT scan images. GM aging features include overall shrinking of the gyri and widening of the sulci, particularly in the medial frontal lobes (axial inset arrows: cingulate sulci), lateral and medial temporal lobes (e.g., Sylvian fissures and temporal opercula), parietal lobes (e.g., parietal opercula), insulae (coronal inset arrows: circular sulci), and hippocampal formations (e.g., choroid fissures and ambient cisterns). WM aging is highlighted by enlargement of CSF structures (lateral and third ventricles) and by brain stem atrophy (sagittal inset arrows: boundary between the pons and medulla oblongata). Cerebellar atrophy (sagittal inset) reflects both GM and WM loss.

**Figure 3.** Neuroanatomic differences between a subject representative of the Tsimane trajectory at age 80 (first row, *cf.* continuous red trace in **Figure 1A**) and a subject representative of the reference trajectory at the same age (second row, *cf.* continuous black trace in **Figure 1A**). Axial, sagittal, and coronal CT slices are shown for each subject. Key neuroanatomic distinctions between the two subjects are highlighted by arrows within each inset and include the extent of atrophy along (A) the circular sulcus of the insula, (B) the precentral and central sulci, and (C) the hippocampal formation.

Figure 1

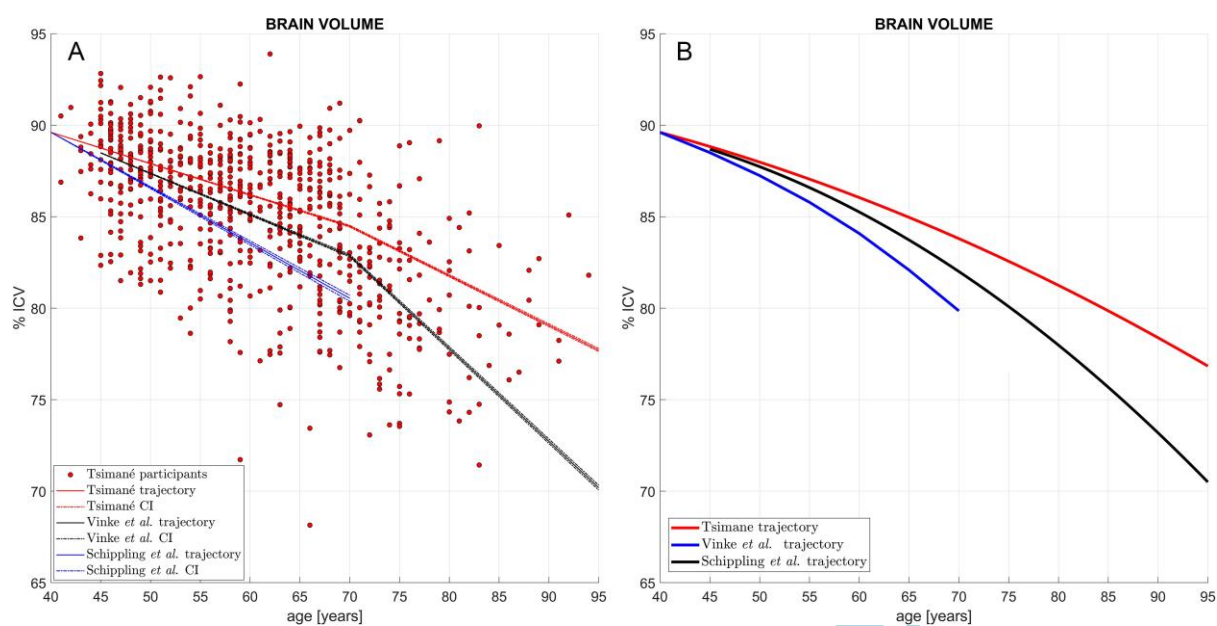


Figure 2

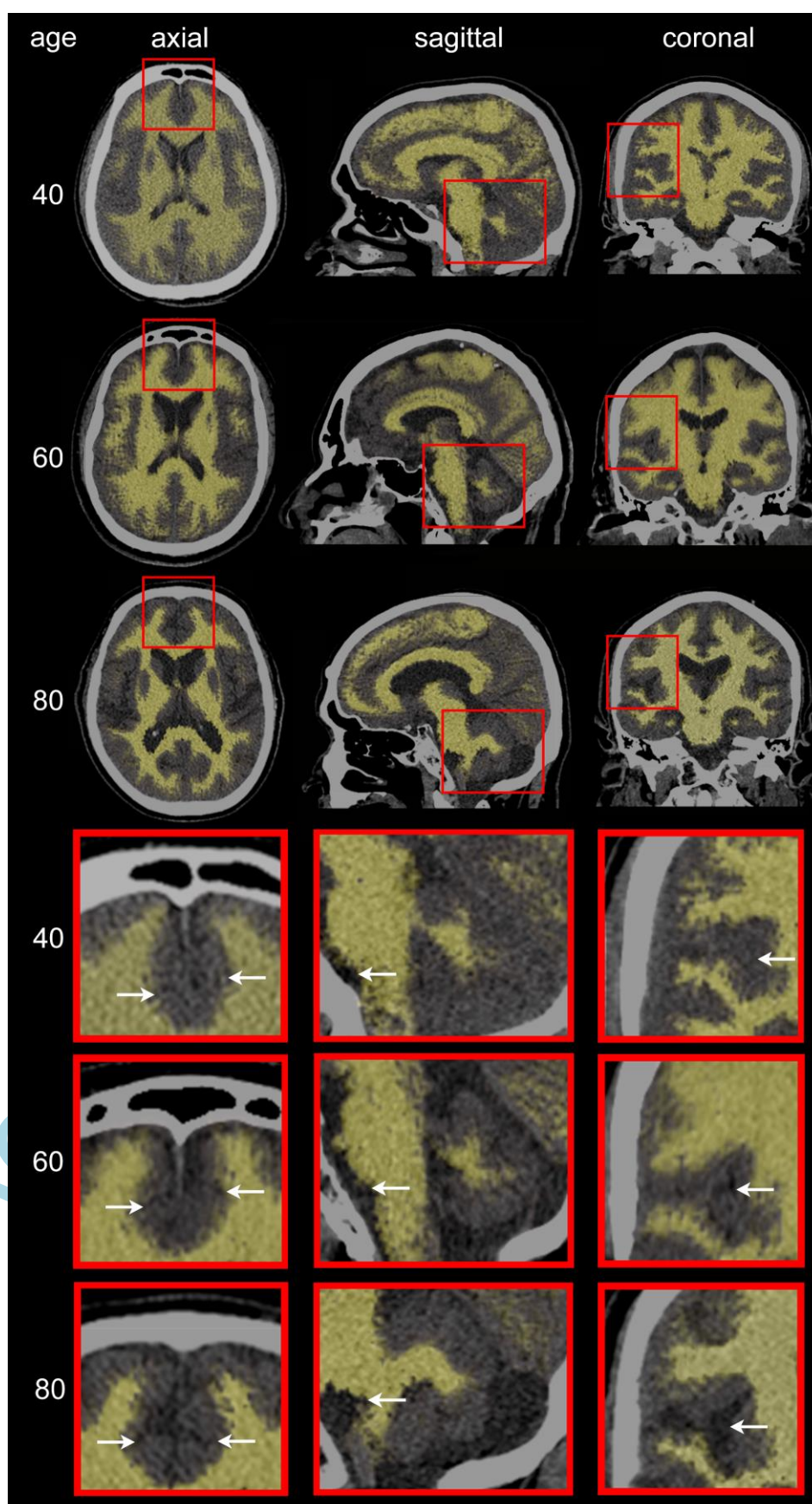




Figure 3

